

Observation of domain structure and coarsening at Cu-Pd alloy vicinal surfaces

S. Goapper, L. Barbier, and B. Salanon

Service de Recherches sur les Surfaces et l'Irradiation de la Matière, CEA/Saclay, 91191 Gif sur Yvette, France

A. Loiseau

Laboratoire d'Etude des Microstructures, ONERA-CNRS, Boîte Postale 72, 92322 Châtillon-sous-Bagneux Cedex, France

X. Torrelles

European Synchrotron Radiation Facility, Boîte Postale 220, 38043 Grenoble Cedex, France

(Received 2 February 1998)

The morphology of a vicinal surface of an A_3B -type ordered alloy [$\text{Cu}_{83}\text{Pd}_{17}(1,1,11)$] is investigated by STM and He diffraction. In the ordered state of the alloy, domains with paired steps are observed and STM images reveal the link between the surface structure and the chemically ordered underlying domains. The surface domain size grows during aging as $t^{1/2}$. The activation energy for this coarsening process is found to be 2.2 eV. This value is close to the one obtained for bulk ordering. [S0163-1829(98)04319-7]

The comprehension of surface microstructures is of fundamental and technological interest as they are expected to play a major role in the related fracture, adhesion, wear, or catalytic properties of solids. In bulk alloys chemical ordering has been investigated for a long time together with its relation with metallurgical properties.¹ Binary alloys that undergo a chemical order-disorder transition (at T_c) on a fixed lattice are of generic interest to perform such studies. In the vicinity of surfaces, concentrations and chemical order at equilibrium are perturbed by segregation,² and reduced coordination of surface atoms gives rise to surface-induced disorder for temperatures close to the transition temperature T_c .^{3,4} Moreover, the kinetics of ordering was found to exhibit original features when taking place near the surface.^{5,6} The trend to chemical ordering is likely to affect dramatically the surface morphology as well. Previous studies of Cu-Pd alloys revealed that the surface equilibrium morphology can be strongly linked to chemical order. Indeed a double step structure was observed below T_c (778 K) (Refs. 7–9) on vicinals of $\text{Cu}_{83}\text{Pd}_{17}$. Moreover, it was found that above T_c (i.e., when long-range chemical order is destroyed) the double step structure on this alloy reverts to a single step one, showing that the surface morphological transition is chemical order driven [8,9]. Indications for double height steps were also found for Cu_3Au .^{10,11}

These A_3B -type alloys exhibit a first-order phase transition from a low- T simple cubic $L1_2$ structure described by a three-component order parameter¹² to a high- T disordered fcc state. As for bulk chemical ordering symmetry breaking leads to the coexistence of 4 translational variants bounded by 3 types of antiphase boundaries (APB's). The density of APB's is further reduced in the subsequent coarsening stage.^{13,14} This latter stage is in fact characterized by a single length scale, the average domain size. For a first-order transition with a nonconserved order parameter this size is expected to follow a $t^{1/2}$ universal behavior according to Lifshitz¹⁵ and Allen-Cahn¹⁶ (LAC).

In this paper we report on direct observations by scanning tunneling microscopy (STM) of the paired step structure on a

vicinal surface of an A_3B -type alloy. For a sample shortly aged below T_c we see domains of paired steps, separated by walls. For step edges we have obtained atomic resolution images that exhibit contrast between Cu and Pd atoms. This allows us to identify unambiguously surface walls with the emergence of APB's. Domains of paired steps on the surface thus give an unprecedented real space picture of chemically ordered domains on the surface of an alloy. We show that STM images allow one to measure the characteristic surface domain size and to follow the coarsening stage of step pairing.

We have chosen to investigate the same vicinal surface of (001) as in Ref. 9 [viz. $\text{Cu}_{83}\text{Pd}_{17}(1,1,11)$],¹⁷ step height $h = 1.83 \text{ \AA}$, step-step distance along $[1\bar{1}0]$ $L_0 = 5.5a$ with $a = 2.59 \text{ \AA}$. For this vicinal surface the ideal bulk truncation would exhibit terraces alternately pure Cu and mixed Cu-Pd. Under ultrahigh vacuum the sample was first Ar^+ bombarded at room temperature (RT) and then annealed above T_c ($T = 873 \text{ K}$) for 1 h to restore surface concentrations. After such a treatment the disordered sample was aged below T_c for chemical ordering and subsequently cooled to RT for STM observations. For long ordering time (48 h at $T_c - 30 \text{ K}$) constant current STM pictures of the surface show double steps separating double width terraces ($2L_0$).⁹ For short ordering time (1 h at $T_c - 30 \text{ K}$) STM images show that step pairing exhibits a domain structure (see Fig. 1). Along line-like zones, which we call surface domain walls (SDW's), steps separate locally to pair differently. Within each domain double steps are rather straight and strongly coupled.

The chemical nature of step edges can be inferred from STM images with atomic resolution. Let us consider the left side of the STM picture in Fig. 2: along the crest of the upper step edge ($A_1 - A_2$) we measured for the tip height modulation period 2.6 \AA , i.e., the crystallographic distance between adjacent atoms a . In contrast, the measured height modulation period along the crest of the lower step edge ($B_1 - B_2$) is 5.2 \AA . This strongly suggests that the terrace ending at ($A_1 - A_2$) is pure copper (period a) whereas the subterrace

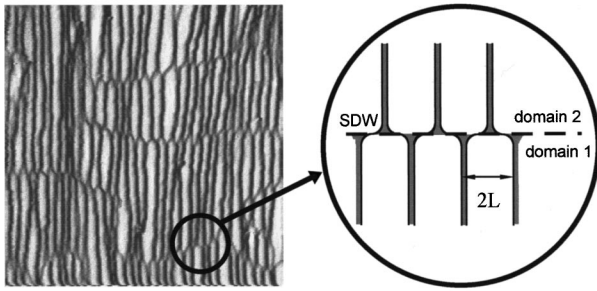


FIG. 1. Left: top view of the gradient of STM tip height across the step direction of the $\text{Cu}_{83}\text{Pd}_{17}(1,1,11)$ surface (after 48 h annealing at $\Delta T = 13$ K, image size $1024 \times 1024 \text{ \AA}^2$). Paired steps are seen as broad dark lines. Right: scheme of a surface domain wall (SDW) at a magnified scale.

atomic plane is mixed Cu-Pd (period $2a$). This is in accordance with the bulk structure and in agreement with ion scattering experiments on the (110) surface of a Cu-Pd alloy.^{18,19} Note that only vicinals of alloys can provide such information on the composition of subsurface crystallographic planes that would be invisible in the case of singular surfaces. The STM picture in Fig. 2 is crossed by a SDW whose step pairing is different on each side. One sees that when crossing the SDW the tip height modulation along the A step edge changes from 2.6 \AA ($A_1 - A_2$) to 5.2 \AA ($A_3 - A_4$). Conversely the tip height modulation along the B step edge changes from 5.2 \AA ($B_1 - B_2$) to 2.6 \AA ($B_3 - B_4$). On the left side of the SDW the terrace plane ending at ($A_1 - A_2$) is Cu while on the right side the very same crystallographic plane becomes a subterrace Cu-Pd one (emerging at the $A_3 - A_4$ step). The chemical composition of (001) atomic planes thus

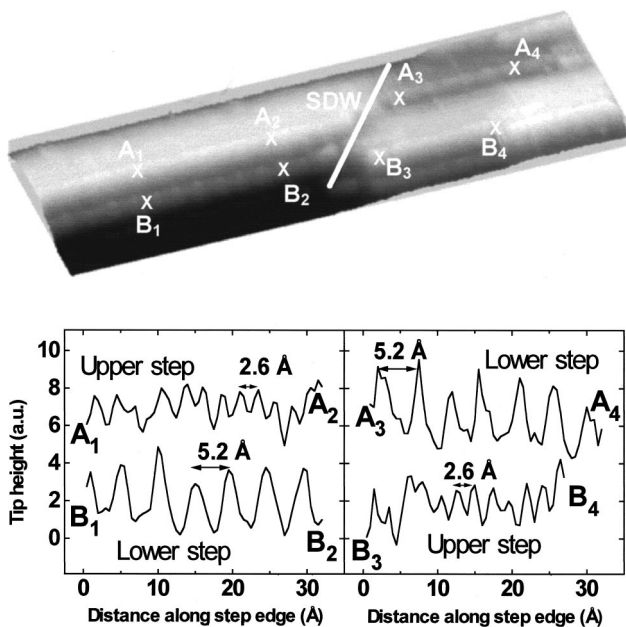


FIG. 2. Perspective view of a $32 \times 128 \text{ \AA}^2$ STM image with atomic resolution along step edges. Heavy white line: SDW. Curves: tip height along the crest of steps A and B . On the left side of the SDW A (B) is an upper (lower) step with a tip height period 2.6 \AA (5.2 \AA , one atom out of two is seen). The reverse is seen on the right side of the SDW.

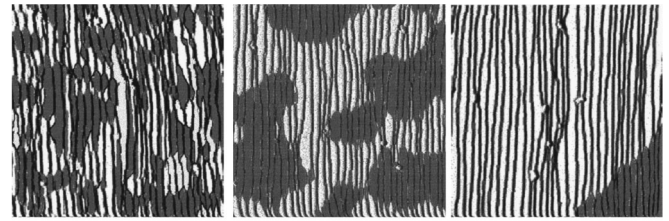


FIG. 3. $1024 \times 1024 \text{ \AA}^2$ STM pictures after, from left to right: 8 min, 1 h, and 48 h annealing at $\Delta T = 13$ K. Grey and white areas are surface domains colored according to step pairing. The analysis of results shows that areas with a given pairing correspond to chemically ordered domains.

changes from Cu to Cu-Pd across SDW's. These boundaries are unambiguously the manifestation of the emergence of APB's involving a phase shift in the Pd concentration profile perpendicular to the terraces. The near surface chemical domain structure is apparent via the step domain structure. As there are only two ways to pair adjacent steps the surface exhibits two variants. Note that only 2 APB's out of the 3 possible ones involve a change in the composition of bulk (001) atomic planes when crossing the boundary²⁰ and can be seen as SDW's.

From large-scale STM images (Fig. 3) the shape of the surface domains can be directly observed. SDW's exhibit no strong preferred orientation, very much like bulk APB's.²¹ We have deduced a characteristic length Λ as follows. We measured the total length L_{SDW} of observable SDW's on several STM images (total surface S). Λ is deduced as $\Lambda = (2S/L_{\text{SDW}})$. In order to follow the kinetics of domain coarsening, we measured Λ for different ordering temperatures below T_c ($\Delta T = T_c - T = 83, 46,$ and 13 K) and ordering times (10^3 to 2×10^5 s). In each case at least 5 pictures (minimum size $512 \times 512 \text{ \AA}^2$) were analyzed. Figure 3 shows typical images for different aging times. The variation of Λ as a function of aging time shown in Fig. 4 is discussed below.

Once the surface morphology of $\text{Cu}_{83}\text{Pd}_{17}(1,1,11)$ is precisely known by STM, it is tempting to use a surface sensitive diffraction probe to follow *in situ* the domain coarsening kinetics at the ordering temperature. We have thus achieved

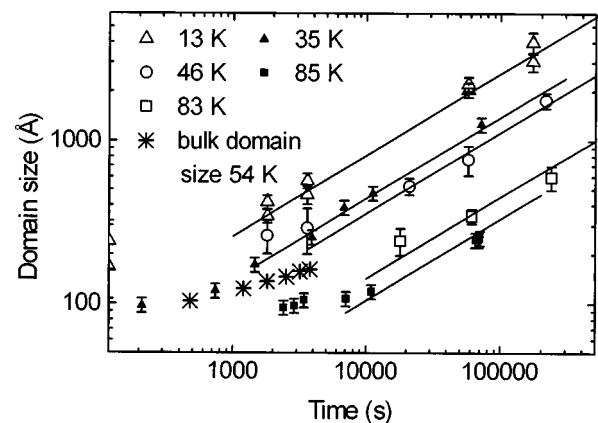


FIG. 4. Domain size vs annealing time at given temperatures indicated by ΔT . Open symbols: STM measurements; Full symbols: He measurements. Lines are best fits with $A(T)t^{1/2}$ law. *: Bulk domain size as determined by x-ray diffraction.

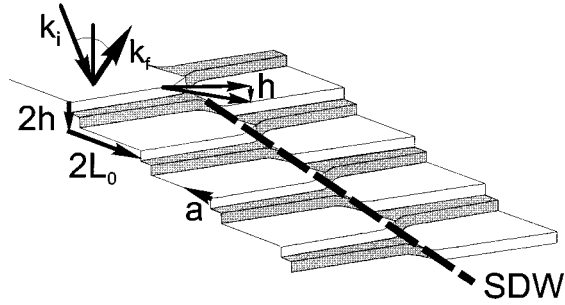


FIG. 5. Schematic perspective view of the surface across a bulk APB, which emerges as a SDW. Step edges with Cu-Pd mixed composition are shaded. h : single step height as well as perpendicular component of the SDW translation vector. k_i and k_f : wave vectors for He diffraction in DSS conditions. a : kink vector at step edges.

thermal energy atom scattering (TEAS) measurements on our sample. As He atoms do not penetrate into the bulk this diffraction technique is highly sensitive to the surface morphology and rather insensitive to differences between Cu and Pd. All measurements were done with the incidence plane perpendicular to the step direction and with wave vector $k_i = 6.4 \text{ \AA}^{-1}$. Diffraction peaks for the ideal double step surface fulfill the Bragg condition $2(\mathbf{L}_0 + \mathbf{h}) \cdot \mathbf{q} = 2m\pi$. $|\mathbf{L}_0| = 5.5a$ is the single terrace width, $|\mathbf{h}|$ is the height of a single step, and \mathbf{q} is the momentum transfer; see Fig. 5. In the presence of SDW's, adjacent domains are translated with respect to each other. The component of the translation vector perpendicular to terraces is \mathbf{h} . In addition to this type of disorder, step edges meander and exhibit kinks of length a . Generally, both contribute to peak broadening. In order for diffraction to be exclusively domain structure sensitive (DSS) we have chosen the incidence angle of the He beam so that an odd order peak ($m=5$) is specular to the terraces and in phase opposition with respect to \mathbf{h} ($\mathbf{h} \cdot \mathbf{q} = m\pi$). The diffraction peak of interest is then sensitive neither to the step disorder nor to the component of the domain shift parallel to the terraces ($\mathbf{q} \perp \mathbf{L}_0$). This diffraction peak is thus selectively sensitive to SDW's. The ($m=5$) peak was scanned perpendicular to the incidence plane and we found that peak broadening is minimum for DSS conditions, as expected. After long aging (48 h at $T_c - 10 \text{ K}$) the peak shape is Gaussian and its width is resolution limited. After a short aging the peak is broadened and its shape is well fitted by an instrument convoluted Lorentzian (width W_L). The characteristic surface domain size was deduced as $\Lambda = (2\pi/W_L)$. Results reported on Fig. 4 show a nice agreement with STM data and are discussed below.

STM ($\Delta T = 13 \text{ K}$) and TEAS ($\Delta T = 35 \text{ K}$) show that Λ follows a $A(T)t^n$ law with $n = 0.5 \pm 0.05$. For shorter times a slower variation is observed, this initial stage being longer for lower temperatures, very much like in bulk Cu_3Au .²² Fitting TEAS and STM late stage data for larger ΔT with $A(T)t^n$ and keeping consistently $n = 1/2$ gives the temperature dependence of the prefactor, which in turn is related to the diffusion constant of the ordering process. The activation energy deduced from an Arrhenius plot of $A(T)$ is $2.25 \pm 0.15 \text{ eV}$ [Fig. 6].

Finally, as morphological domains coincide with chemically ordered domains, it is of interest to compare our values

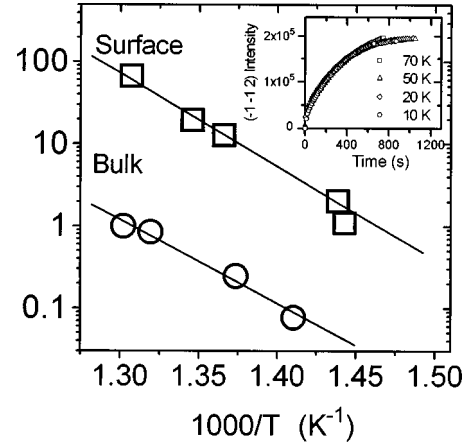


FIG. 6. Arrhenius diagram for (\square) square of the prefactor $A(T)$ ($\text{\AA}^2 \text{ s}^{-1}$) of $t^{1/2}$ for Λ . Full line is best fit (activation energy = $2.25 \pm 0.15 \text{ eV}$). (\circ) time scaling factor (unity for $\Delta T = 10 \text{ K}$) of the $(\bar{1}\bar{1}2)$ peak intensity (activation energy = $2.0 \pm 0.15 \text{ eV}$). Inset: Time scaling of the x-ray diffraction peak intensity (counts) after quenching from above T_c to given ΔT . Time scale is for $\Delta T = 10 \text{ K}$.

of domain size and activation energy for surface domain coarsening with corresponding values for bulk chemical ordering. For this purpose we have used x-ray data taken at ESRF on the very same sample. Bulk ordering kinetics at constant T was followed by measuring versus time the $(\bar{1}\bar{1}2)$ bulk chemical order diffraction peak (bulk DSS condition). The incidence angle (0.3°) was above the critical angle $\alpha_c = 0.27^\circ$. We found that the central peak intensity variation after quenches from above T_c to $\Delta T = 70, 50, 20$, and 10 K can be time scaled (see Fig. 6-inset). An Arrhenius plot of the time scaling factors gives a bulk ordering activation energy of $2.0 \pm 0.15 \text{ eV}$, very close to the measured surface value. From peak width scaling measurements for $\Delta T = 54 \text{ K}$ ($t = 500$ to $3 \times 10^3 \text{ s}$) we have determined the corresponding bulk characteristic length [note that 2 APB's out of 3 contribute to the broadening of the $(\bar{1}\bar{1}2)$ bulk peak]. Results reported in Fig. 4 are of the same order as the surface domain sizes measured by STM or TEAS. Note that from the variation of bulk domain size measured for short times ($t < 1 \text{ h}$) one cannot extrapolate the value of the late stage exponent.

In summary, we have shown that the morphological resolution of STM allows one to explore surface chemical ordering via step arrangements and to follow kinetics. Within experimental errors the size of bulk domains and that of surface domains turn out to be similar, this is also true when comparing bulk and surface activation energies. The value of the time exponent n for surface domains is compatible with the LAC formalism.

Our prime result is the visualization of the emergence of APB's at the surface. This observation is in contrast with recent results on $\text{Cu}_3\text{Au}(001)$, for which Reichert *et al.*⁶ reported that no APB's involving a phase shift in the Au concentration profile perpendicular to the surface are created in the near surface region during ordering. These authors explain this observation as due to the oscillatory segregation profile present above T_c ,²³ which acts as a template for chemical ordering, thus pointing out a surface specific ordering effect not seen here. For our Cu-Pd vicinal surface these very APB's are apparent on STM images. The two systems

are indeed different in several aspects. Note first that APB's in Cu_3Au are strongly anisotropic [conservative (001)], in contrast with APB's in Cu-Pd, which exhibit no preferred orientation, this could induce changes in the localization of APB's near the surface. Most importantly, for a vicinal surface, segregation effects on neighboring terraces act in phase opposition so that on the average possible template effects

are canceled. Whether it is the presence of steps or a difference between the two alloys that brings about these contrasting behaviors it is clear here that the surface morphology reflects the subsurface chemical order.

We would like to thank S. Clausse for his help in performing the STM experiments. We are greatly indebted to the Surface Diffraction group at ESRF.

-
- ¹J. D. Gunton, M. San Miguel, and P. S. Sahni, in *Phase Transitions and Critical Phenomena*, Vol. 8, edited by C. Domb and J. L. Lebowitz (Academic Press, London, 1983).
- ²See, e.g., J. Tersoff, *Phys. Rev. B* **42**, 10 965 (1990), and references therein.
- ³R. Lipowsky and W. Speth, *Phys. Rev. B* **28**, 3983 (1983).
- ⁴H. Dosch, L. Mailänder, A. Lied, J. Peisl, F. Grey, R. L. Johnson, and S. Krummacher, *Phys. Rev. Lett.* **60**, 2382 (1988); L. Mailänder, H. Dosch, J. Peisl, and R. L. Johnson, *ibid.* **64**, 2527 (1990).
- ⁵E. G. McRae and R. A. Malic, *Phys. Rev. Lett.* **65**, 737 (1990); *Phys. Rev. B* **42**, 1509 (1990).
- ⁶H. Reichert, P. J. Eng, H. Dosch, and I. K. Robinson, *Phys. Rev. Lett.* **78**, 3475 (1997).
- ⁷L. Barbier, B. Salanon, and A. Loiseau, *Phys. Rev. B* **50**, 4929 (1994).
- ⁸S. Goapper *et al.* (unpublished).
- ⁹L. Barbier, S. Goapper, B. Salanon, R. Caudron, A. Loiseau, J. Alvarez, S. Ferrer, and X. Torrelles, *Phys. Rev. Lett.* **78**, 3003 (1997).
- ¹⁰H. Niehus and C. Achete, *Surf. Sci.* **289**, 19 (1993).
- ¹¹E. G. McRae, T. M. Buck, R. A. Malic, W. E. Wallace, and J. M. Sanchez, *Surf. Sci.* **238**, L481 (1990).
- ¹²F. Ducastelle, *Order and Phase Stability in Alloys (Vol. 3 Cohesion and Structure)* (North-Holland, Amsterdam, 1991).
- ¹³S. E. Nagler, R. F. Shannon, C. R. Harkless, and M. A. Singh, *Phys. Rev. Lett.* **61**, 718 (1988).
- ¹⁴R. F. Shannon, S. E. Nagler, C. R. Harkless, and R. M. Nicklow, *Phys. Rev. B* **46**, 40 (1992).
- ¹⁵I. M. Lifshitz, *Zh. Eksp. Teor. Phys.* **42**, 1354 (1962) [*Sov. Phys. JETP* **15**, 939 (1962)].
- ¹⁶S. M. Allen and J. W. Cahn, *Acta Metall.* **27**, 1085 (1979).
- ¹⁷Note that the composition of the sample was chosen in order to correspond to the congruent point in the bulk phase diagram.
- ¹⁸M. A. Newton, S. M. Francis, Y. Li, D. Daw, and M. Bowker, *Surf. Sci.* **259**, 45 (1991).
- ¹⁹R. H. Bergmans, M. Van de Grift, A. W. Denier van der Gon, and H. H. Brongersma, *Surf. Sci.* **345**, 303 (1996).
- ²⁰L. Potez and A. Loiseau, *Interface Sci.* **2**, 91 (1994).
- ²¹C. Ricolleau, A. Loiseau, F. Ducastelle, and R. Caudron, *Phys. Rev. Lett.* **68**, 3591 (1992).
- ²²T. Hashimoto, K. Nishimura, and Y. Takeuchi, *Phys. Lett.* **65A**, 250 (1978).
- ²³H. Reichert, P. J. Eng, H. Dosch, and I. K. Robinson, *Phys. Rev. Lett.* **74**, 2006 (1995).